Prion Protein Binds Copper within the Physiological Concentration Range

Kramer, Michael L ; Kratzin, Hartmut D ; Schmidt, Bernhard ; Römer, Alice ; Windl, Otto ; Liemann, Susanne ; Hornemann, Simone ; Kretzschmar, Hans

Abstract: The prion protein is known to be a copper-binding protein, but affinity and stoichiometry data for the full-length protein at a physiological pH of 7 were lacking. Furthermore, it was unknown whether only the highly flexible N-terminal segment with its octarepeat region is involved in copper binding or whether the structured C-terminal domain is also involved. Therefore we systematically investigated the stoichiometry and affinity of copper binding to full-length prion protein PrP23–231 and to different N- and C-terminal fragments using electrospray ionization mass spectrometry and fluorescence spectroscopy. Our data indicate that the unstructured N-terminal segment is the cooperative copper-binding domain of the prion protein. The prion protein binds up to five copper(II) ions with half-maximal binding at 2 m. This argues strongly for a direct role of the prion protein in copper metabolism, since it is almost saturated at about 5 m,and the exchangeable copper pool concentration in blood is about 8 m.

DOI: https://doi.org/10.1074/jbc.m006554200

THE JOURNAL OF BIOLOGICAL CHEMISTRY
Vol. 276, No. 20, Issue of May 18, pp. 16711–16719, 2001

Printed in U.S.A.

Prion Protein Binds Copper within the Physiological Concentration Range*

Received for publication, July 24, 2000, and in revised form, February 21, 2001
Published, JBC Papers in Press, February 27, 2001, DOI 10.1074/jbc.M006554200

Michael L. Kramer‡§, Hartmut D. Kratzin¶, Bernhard Schmidt‖, Alice Römer‡, Otto Windl‡, Susanne Liemann‡‡, Simone Hornemann§§, and Hans Kretzschmar‡****

From the ‡Department of Neuropathology, Georg August University of Göttingen, Robert-Koch-Strasse 40, 37075 Göttingen, Germany, the ¶Department of Immunochemistry, Max-Planck Institute for Experimental Medicine, Hermann-Rein-Strasse 3, 37075 Göttingen, Germany, the ‖Department of Biochemistry II, Georg August University of Göttingen, Heinrich-Düker-Weg 12, 37073 Göttingen, Germany, the ‡‡Laboratory of Molecular Medicine, Children's Hospital, Boston, Massachusetts 02115, and the §§Institute of Molecular Virology, GSF-Center for Environmental and Health Research, Technical University of Munich, Trogerstrasse 4b, 81675 München, Germany

The prion protein is known to be a copper-binding protein, but affinity and stoichiometry data for the full-length protein at a physiological pH of 7 were lacking. Furthermore, it was unknown whether only the highly flexible N-terminal segment with its octarepeat region is involved in copper binding or whether the structured C-terminal domain is also involved. Therefore we systematically investigated the stoichiometry and affinity of copper binding to full-length prion protein $PrP_{23–231}$ and to different N- and C-terminal fragments using electrospray ionization mass spectrometry and fluorescence spectroscopy. Our data indicate that the unstructured N-terminal segment is the cooperative copper-binding domain of the prion protein. The prion protein binds up to five copper(II) ions with half-maximal binding at ~2 μM. This argues strongly for a direct role of the prion protein in copper metabolism, since it is almost saturated at about 5 μM, and the exchangeable copper pool concentration in blood is about 8 μM.

Prion diseases are fatal neurodegenerative diseases thought to be caused by conformational transition of the native and predominantly α-helical prion protein (PrP^C)[1] to the significantly more β-sheet-containing pathogenic isoform (PrP^{Sc}) (1). This conformational transition apparently induces the formation of PrP^{Sc} aggregates (2), which are, in contrast to PrP^C, highly protease-resistant (3). During infection, PrP^{Sc} appears to serve as a template for the conversion of the native prion protein, because host PrP^C expression is required for infection with prions (4). There is evidence that copper plays a role in the formation of PrP^{Sc} (5).

PrP^C is nearly ubiquitously distributed to all tissues. The highest levels are found in the brain (6). Native PrP^C is an asparagine-linked sialoglycoprotein that is attached to the surface of the plasma membrane via a C-terminal glycophosphatidylinositol anchor (7). The structured C-terminal half of the full-length recombinant $PrP_{23–231}$ (amino acids 23–231) from amino acids 126–231 is made up of two strands of one small antiparallel β-sheet and three α-helices (8). The N-terminal half from amino acids 23–125 showed no structure in NMR analysis and is therefore postulated to be highly flexible (9, 10).

Although many efforts have been made the physiological function of PrP^C has not yet been identified (11, 12). In 1995 it was suggested that the octarepeat region ($[PHGGGWGQ]_4$) from amino acids 60–91 within the flexible N-terminal half of the prion protein may play a role in binding copper (13). We have shown that PrP^C has indeed a function in synaptic copper binding (14). Heavy metal binding studies indicated that PrP^C seems to specifically bind copper (15). Half-maximal binding of two copper ions at 14 μM was reported for Syrian hamster $Sham PrP_{29–231}$ at pH 6.0 (15). In contrast, binding of 4 and 5.6 copper ions to the octarepeat region peptide (16, 17) and $hum PrP_{23–98}$ (18) at pH 7.4 with half-maximal binding at about 6 μM were found, respectively. The copper binding to the octarepeat region was shown to be strongly pH-dependent in the range from 5 to 7 (14) with almost no binding at pH 5.

The lack of affinity and stoichiometry data for the full-length prion protein at a physiological pH of 7, as well as the question of which part of the prion protein is responsible for the copper binding, prompted us to systematically investigate the copper binding to the full-length prion protein as well as to different N- and C-terminal fragments using fluorescence spectroscopy and electrospray ionization mass spectrometry.

In this paper we present for the first time copper binding data on the full-length prion protein under physiological conditions at pH 7. Our data show that the prion protein binds up to five copper ions and is almost saturated at 5 μM copper(II). Furthermore, our data suggest that the highly flexible N-terminal half is the cooperative copper-binding domain of the prion protein.

EXPERIMENTAL PROCEDURES

Materials and Reagents—MOPS, dodecyltrimethylammonium chloride, $CuSO_4 \cdot 5H_2O$, and *N*-ethylmorpholine were purchased from Fluka (Deisenhofen, Germany). Chelite P was obtained from Serva (Heidelberg, Germany). Ion exchange matrices EMD-COOH, EMD-TMAE, and thrombin were ordered from Merck (Darmstadt, Germany). All other reagents used were of analytical grade.

Synthesis and Purification of $humPrP_{60–91}$ and $humPrP_{60–109}$—The peptides $hum PrP_{60–91}$ and $hum PrP_{60–109}$ were synthesized on an 9050-peptide synthesizer (Millipore) using amino acids protected with Fmoc (1-fluorenylmethoxycarbonyl) and activated with benzotriazol-1-yl-oxy-

* This work was supported by the European Union Grant BMH4-CT98-6051, by the BMBF of Germany, and by a grant from the Boehringer Ingelheim Fonds (to S. H.). The costs of publication of this article were defrayed in part by the payment of page charges. This article must therefore be hereby marked "*advertisement*" in accordance with 18 U.S.C. Section 1734 solely to indicate this fact.

§ To whom correspondence should be addressed: Tel.: 49-551-39-2700; Fax: 49-551-39-8472; E-mail: mkramer@med.uni-goettingen.de.

** Present address: Ludwig Maximilian University, Dept. of Neuropathology, Marchionini-Str. 17, 81377 München, Germany.

[1] The abbreviations used are: PrP, prion protein; ESI, electrospray ionization; MOPS, 4-morpholinepropanesulfonic acid; DTAC, dodecyltrimethylammonium chloride; NEMO, *N*-ethylmorpholine; HPLC, high performance liquid chromatography; amu, average mass unit; MS, mass spectrometry.

TABLE I
Molecular masses for the copper binding of the prion protein and its fragments calculated from ESI mass spectra

Peptide/Protein	Mass (amu)	Δm (amu)
*hum*PrP$_{60-91}$	3125.0 ± 0.1	
	3187.1 ± 0.5	62.1
	3248.3 ± 0.1	61.2
	3309.6 ± 0.3	61.3
	3371.4 ± 0.2	61.8
		Average = 61.6
*hum*PrP$_{60-109}$	5061.9 ± 0.5	
	5123.4 ± 2.0	61.5
	5184.5 ± 0.7	61.1
	5246.3 ± 0.5	61.8
	5306.8 ± 0.6	60.5
	5367.4 ± 1.1	60.6
		Average = 61.1
*hum*PrP$_{23-98}$	7813.0 ± 0.8	
	7873.9 ± 1.7	60.9
	7936.4 ± 1.2	62.5
	7998.1 ± 1.2	61.7
	8059.2 ± 1.2	61.1
	8121.2 ± 1.2	61.9
	8184.0 ± 0.6	62.8
		Average = 61.8
*hum*PrP$_{23-112}$	9355.4 ± 0.3	
	9416.6 ± 0.9	61.2
	9478.4 ± 0.6	61.8
	9540.3 ± 0.7	61.9
	9600.5 ± 0.8	60.1
	9660.8 ± 1.5	60.3
		Average = 61.1
*mur*PrP$_{121-231}$	13335.5 ± 0.7	
	13397.3 ± 1.5	Average = 61.8
*mur*PrP$_{23-231}$	23110.6 ± 3.1	
	23171.9 ± 2.1	61.3
	23233.7 ± 3.8	61.8
	23294.5 ± 4.3	60.8
	23355.7 ± 2.7	61.2
	23418.2 ± 2.8	62.5
		Average = 61.5

tris(pyrrolidino)phosphonium-hexafluorophoshpate (PyBOP) (19). After cleavage from resin and removal of protecting groups, peptides were first purified by reversed-phase HPLC using a 1.9 × 30-cm^2 Delta Pac C18 column (Millipore) with a gradient from 0 to 50% acetonitrile including 0.1% trifluoroacetic acid for 50 min. Both peptides were further purified on an EMD-COOH column eluting with a gradient from 0.02 to 1 M ammonium acetate, pH 5.0. Finally, peptides were purified by reversed-phase HPLC on a Vydac C_4 column (4 × 250 mm) using a linear water acetonitrile gradient of 10–50% acetonitrile including 0.1% trifluoroacetic acid.

Expression and Purification of Full-length murPrP$_{23-231}$ and N-terminal Fragments humPrP$_{23-98}$ and humPrP$_{23-112}$—The N-terminal fragment *hum*PrP$_{23-98}$ was expressed in *E. coli* according to Brown *et al.* (18). After expression and thrombin cleavage of the GST-*hum*PrP$_{23-98}$ fusion protein, the reaction mixture was applied to an EMD-COOH column and *hum*PrP$_{23-98}$ was eluted with a gradient from 0 M up to 1 M ammonium acetate pH 6.0.

The plasmid pEThuPrP$_{23-112}$ was constructed for the expression of *hum*PrP$_{23-112}$ following the cloning of the human PRNP ORF from genomic DNA (20). The coding region of the N-terminal segment of PrP (aa 23 to 112) was amplified via PCR under standard conditions using primers huPrP23–112up (5′-GGCCGGTCATGAAGAAGCGCCCGAAGCCT-3′) and huPrP23–112do (5′GCCGGGAATTCTTATCACATGTGCTTCATGTTGGT-3′). Primer huPrP23–112up contains a *Bsp*HI cleavage site and a start codon. Primer huPrP23–112do contains two stop codons and an *Eco*RI cleavage site. The construct was cloned into the *Nco*I and *Eco*RI sites of the inducible expression vector pET-21d (Novagen) and the sequence of the insert was verified by DNA sequence analysis

The expression of the *hum*PrP$_{23-112}$ in *E. coli* was induced with IPTG. Harvested cells were lysed with 1% Triton X-100 and centrifuged at 18,500 g for 15 min. The supernatant was applied to an EMD-COOH column, washed with 10 mM ammonium acetate pH 6.0. *hum*PrP$_{23-112}$ and eluted with a linear gradient up to 1 M ammonium acetate pH 6.0 from the column.

Finally, both N-terminal PrP fragments were purified by reversed phase HPLC on a Vydac C_4 column (4 mm x 250 mm) using a linear water acetonitrile gradient of 10% to 50% acetonitrile including 0.1% trifluoroacetic acid.

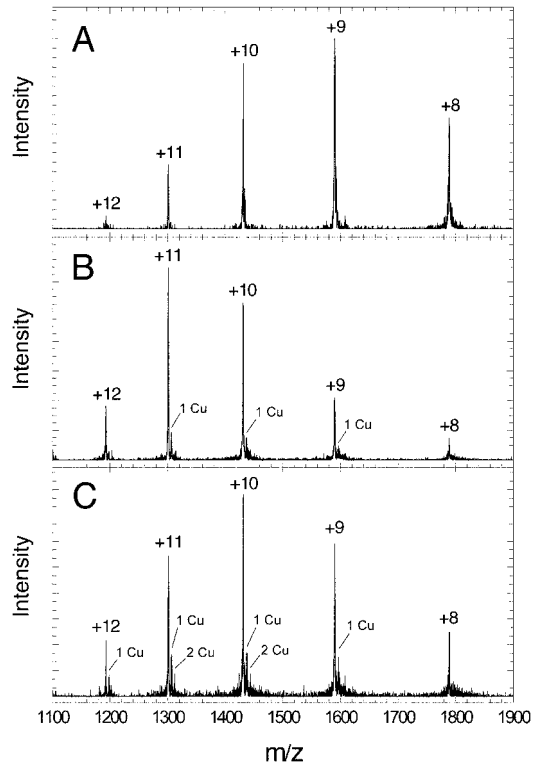

FIG. 1. **ESI mass spectra of hen egg lysozyme with and without copper(II) as negative control.** To 10 μM lysozyme (*A*) at pH 7.4, 50 μM (*B*) and 100 μM (*C*) copper sulfate were added, respectively.

The full-length *mur*PrP$_{23-231}$ was expressed and purified according to Liemann *et al.* (21). Before lyophilization, protein was dialyzed with Chelite P to remove traces of bound copper. The C-terminal fragment *mur*PrP$_{121-231}$ was expressed and purified as described earlier (22).

Fluorescence Titration of PrP$_{23-231}$ and Its Fragments—Fluorescence spectroscopy was carried out on an LS 50B from PerkinElmer Life Sciences (Überlingen, Germany). Measurements were performed in 20 mM MOPS, pH 7.2, 100 mM NaCl, and 1 mM DTAC. MOPS buffer was treated with Chelite P to remove traces of heavy metal ions. To excite selectively tryptophan fluorescence, a wavelength of 295 nm was chosen, and the fluorescence signal was detected on the emission side at 355 nm. Excitation slit width varied from 3 to 5 nm, and emission slit width was in the range of 10–15 nm. For reasons of sensitivity the excitation wavelength for *mur*PrP$_{121-231}$ was set to 285 nm. Copper sulfate was added carefully to prevent possible precipitation (monitored by systematic excitation peak broadening in the emission spectra). Each point in the fluorescence titration curves represents the average of at least three measurements. Fluorescence titrations were performed at 20 °C. Due to absorption of copper in the UV range, fluorescence titration curves were corrected for inner filter effect (23). All curves were corrected for background fluorescence.

ESI Mass Spectrometry—Mass spectrometry of N-terminal PrP fragments with and without copper were performed on a TSQ7000 (Finnigan) in the nano spray mode. The buffer was 1 mM NEMO/formic acid at pH 7.4. The applied spray voltage was 0.8–1.0 kV. Capillary temperature was set to 150 °C.

Peptide and Protein Quantification—Peptide and protein concentrations were determined in 6 M guanidinium chloride according to Gill and von Hippel (24). Peptide quantification by amino acid analysis for *hum*PrP$_{60-91}$ resulted in identical values.

RESULTS

Electrospray Ionization Mass Spectrometry of Full-length PrP$_{23-231}$ and Its Fragments with Copper—ESI mass spectrometry was used to elucidate the stoichiometry of copper binding to the different N-terminal fragments *hum*PrP$_{60-91}$, *hum*PrP$_{60-109}$, *hum*PrP$_{23-98}$, and *hum*PrP$_{23-112}$ as well as for the C-terminal fragment *mur*PrP$_{121-231}$ and for the full-length

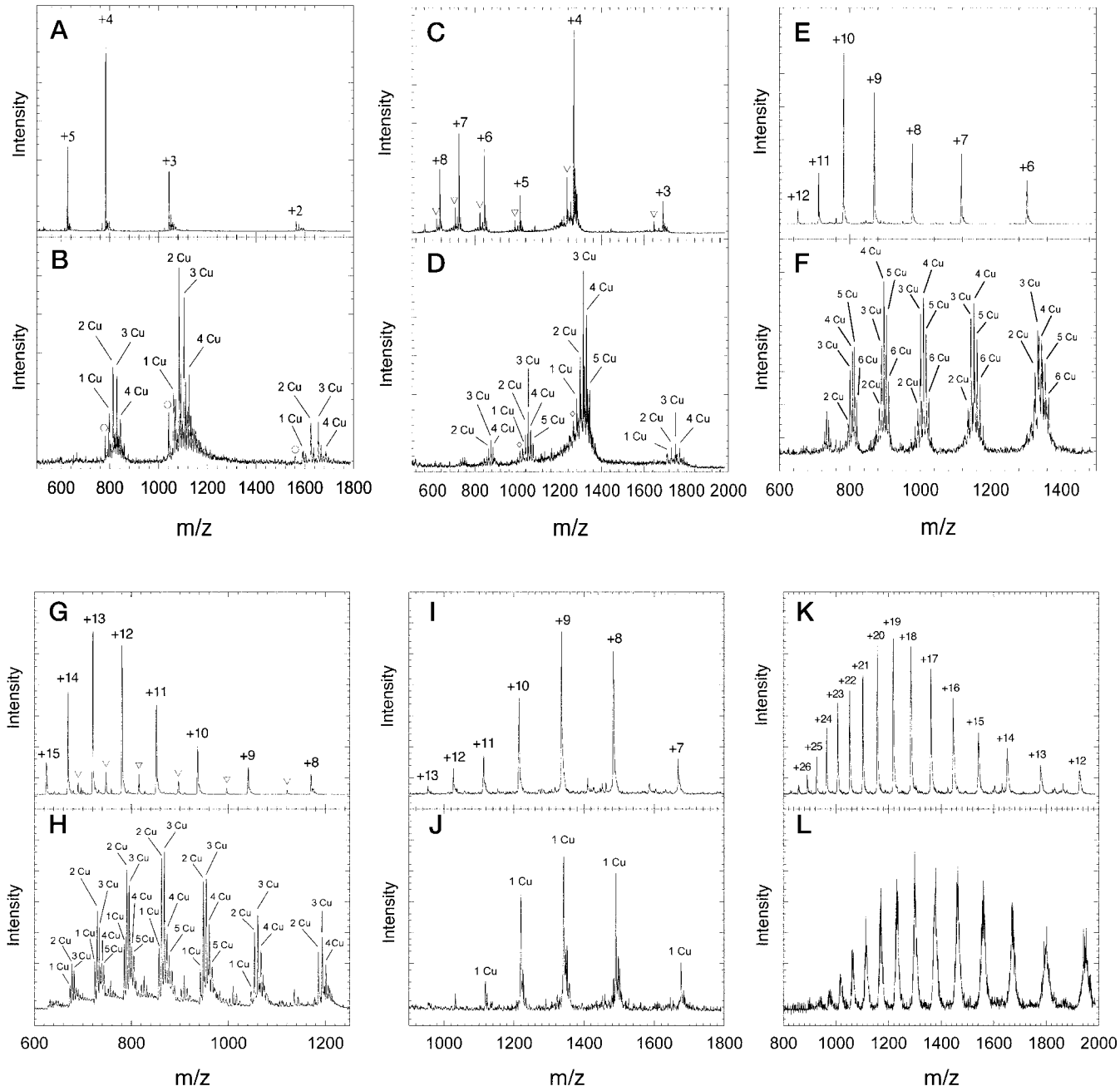

FIG. 2. **ESI mass spectra of PrP^{C} and its fragments with and without copper(II) at pH 7.4.** *A*, *C*, *E*, *G*, *I*, and *K* show the mass spectra of the apopeptides/proteins of *hum*PrP$_{60-91}$, *hum*PrP$_{60-109}$, *hum*PrP$_{23-98}$, *hum*PrP$_{23-112}$, *mur*PrP$_{121-231}$, and *mur*PrP$_{23-231}$. *B*, *D*, *F*, *H*, *J*, and *L* represent the mass spectra of the corresponding holopeptides of 20 μM *hum*PrP$_{60-91}$, 10 μM *hum*PrP$_{60-109}$, 10 μM *hum*PrP$_{23-98}$, 10 μM *hum*PrP$_{23-112}$, 13 μM *mur*PrP$_{121-231}$, and 10 μM *mur*PrP$_{23-231}$ with 100 μM copper(II) and 70 μM copper(II) for *hum*PrP$_{23-98}$, respectively. If present, *open circles* indicate m/z peaks for the apopeptides. The *triangles* in *C* and *G* mark the m/z peaks of by-products (see "Results"). The *diamonds* in *D* mark the m/z peaks for two copper ions bound to the by-product and not for the apopeptide of *hum*PrP$_{60-109}$.

prion protein *mur*PrP$_{23-231}$. The experimental conditions for metal interaction studies at pH 7.4 with respect to suitable buffers and additives were intensively investigated. Finally, we introduced *N*-ethylmorpholine at pH 7.4 as a new buffer system for metal interaction studies with ESI MS, because it did not interfere with copper binding to peptides and protein compared with ammonium salt-containing buffers. Furthermore, addition of solvents like acetonitrile or methanol significantly affected the copper population in the ESI mass spectra (data not shown) and were therefore omitted. To avoid unspecific binding the copper concentration as well as the peptide concentration were kept as low as possible.

For a negative control experiment we used hen egg lysozyme, since it is similar to the prion protein with respect to its size and isoelectric point. Besides the potential unspecific copper binding sites at the N-terminal amino group as well as C-terminal and side chain carboxyl groups, it has one histidine at amino acid position 15 just after the first helix, which is exposed to the solvent. As clearly shown in the spectra of lysozyme with (Fig. 1, *B* and *C*) and without copper (Fig. 1*A*), even at a 10-fold excess of free copper(II) no significant binding occurred. For the first and second copper adduct mass differences of 61.7 and 61.3 average mass units were obtained, respectively. The low unspecific copper binding to lysozyme as a negative control demonstrated that NEMO is an excellent new buffer system for copper interaction experiments with proteins at a physiological pH of 7.

ESI mass spectrometry of the N-terminal fragments (Fig. 2)

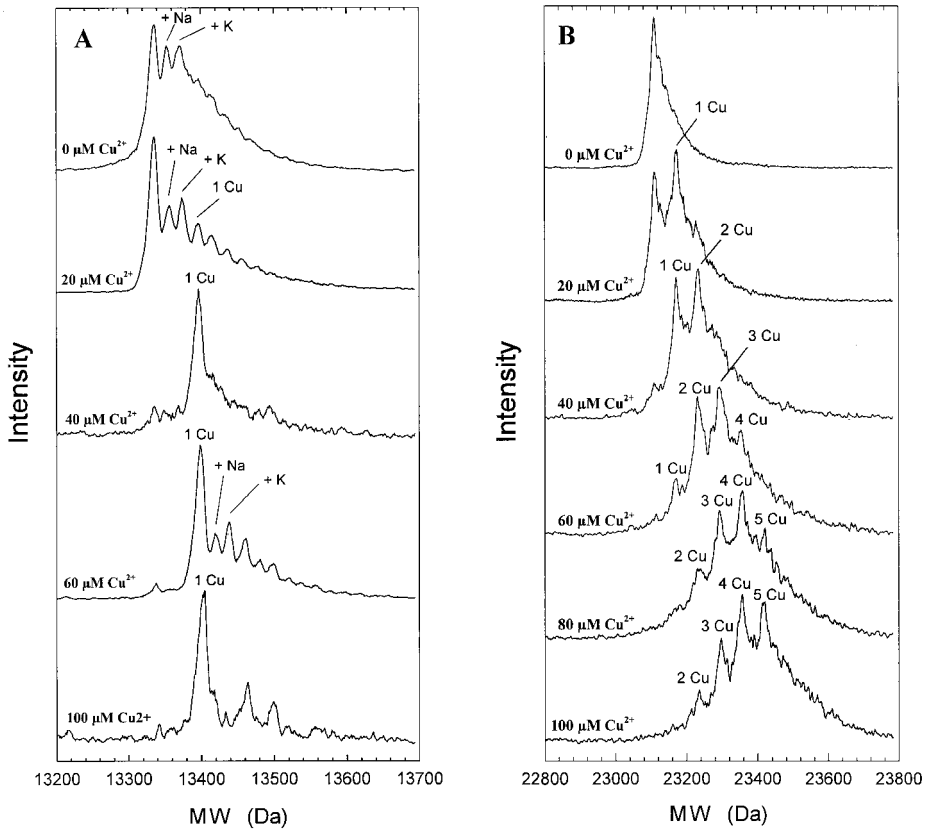

FIG. 3. **Deconvoluted ESI mass spectra of *mur*PrP$_{121–231}$ (*A*) and *mur*PrP$_{23–231}$ (*B*) at different copper concentrations (see the labeling of curves).** The concentrations of *mur*PrP$_{121–231}$ and *mur*PrP$_{23–231}$ were 13 and 10 μM, respectively. Peaks labeled with *Cu*, *K*, and *Na* represent the corresponding adducts for copper, sodium, and potassium.

resulted in the expected average masses for the apopeptides of *hum*PrP$_{60–91}$, *hum*PrP$_{60–109}$, and *hum*PrP$_{23–98}$ (Table I). In the spectrum of apo *hum*PrP$_{60–109}$, a by-product (Fig. 2*C*, marked with *triangles*) with a corresponding mass of 4934.3 amu is observed. The mass difference of 127.6 suggests a missing lysine or glutamine residue in the by-product. The mass calculated from the spectrum of *hum*PrP$_{23–112}$ (Fig. 2*G*) was 1 amu higher than the theoretically expected 9354.2 amu. This is probably due to the hydrolysis of Asn^{108} to Asp^{108} (25). The same holds for the by-product (marked with *triangles*) for which a mass of 8958.6 amu was obtained. The mass difference indicated that the three C-terminal amino acids KHM after Met^{109} have been cleaved off from *hum*PrP$_{23–112}$.

Adding a 5–10-fold excess of copper(II) to the apopeptides resulted in mass spectra (Fig. 2, *B*, *D*, *F*, and *H*) with several copper adduct peaks. On addition of 100 μM copper sulfate to 20 μM *hum*PrP$_{60–91}$, new m/z peaks appeared (Fig. 2*B*) corresponding to up to four bound copper(II) per peptide molecule. The two small peaks between the two following m/z copper peaks are always due to unspecific sodium and potassium adducts commonly observed in mass spectrometry of peptides and proteins at neutral pH. Adding 100 μM copper(II) to 10 μM *hum*PrP$_{60–109}$ resulted in the appearance of additional m/z peaks due to the complex formation of up to five bound copper per *hum*PrP$_{60–109}$ (Fig. 2*D*). Note that the peaks apparently corresponding to zero (marked by *diamonds*) and one bound copper for *hum*PrP$_{60–109}$ are also the main peaks for the by-product with two and three bound copper, because their masses differ only by 4 amu and thus appeared as poorly resolved double peaks. Addition of 70 μM copper(II) to 10 μM *hum*PrP$_{23–98}$ (Fig. 2*F*) led to the appearance of m/z peaks for up to six bound copper ions. It should be noted that adding a 10-fold excess (data not shown) above all significantly raised the intensity of the m/z peaks for six bound copper ions, suggesting a less specific copper binding site. In contrast, only adduct peaks for up to five bound copper were observed on addition of 100 μM copper sulfate to 10 μM of the 14 amino acids longer *hum*PrP$_{23–112}$ (Fig. 2*H*). The significant shift of m/z peaks to lower charge values z and thus higher m/z values on addition of copper suggests conformational changes associated with copper binding, resulting in a more folded or structured conformation compared with the apopeptides.

The structured C-terminal domain of the prion protein *mur*PrP$_{121–231}$ was analyzed by ESI mass spectrometry (Fig. 2*I*) and yielded a mass of 13335.5, which corresponds to the expected average molecular weight of 13334.8. On addition of up to 100 μM copper to 13 μM protein, only one bound copper was observed (Fig. 2*J*). This could be seen easier from the deconvoluted spectra (Fig. 3*A*). This site appears to be of lower affinity, because at 20 μM copper(II), which is the 1.5-fold excess in copper, only a peak of little intensity is observed. At 40 μM copper (a 3-fold excess of copper) the apoprotein peak almost disappeared, and the molecular weight peak for one bound copper became prominent. This remained almost unchanged, increasing the copper concentration up to 100 μM and indicating that there is probably one copper-binding site with lower affinity in *mur*PrP$_{121–231}$. In contrast to the N-terminal fragments, there is no shift of the m/z charge envelope to lower values. Thus, presumably no conformational change occurs on binding of the copper ion.

From the mass spectrum of the apoprion protein *mur*PrP$_{23–231}$ (Fig. 2*K*) an average mass of 23110.6 with a S.D. of 3.1 is obtained, which is about 6 amu higher than the expected molecular mass of 23104.4. The reason for this difference was unclear. On addition of up to 100 μM copper, several not very well resolved copper adduct peaks (Fig. 2*L*) appeared. Due to the broad half-peak width and the high charges, the copper adduct peaks could be observed better from the deconvoluted

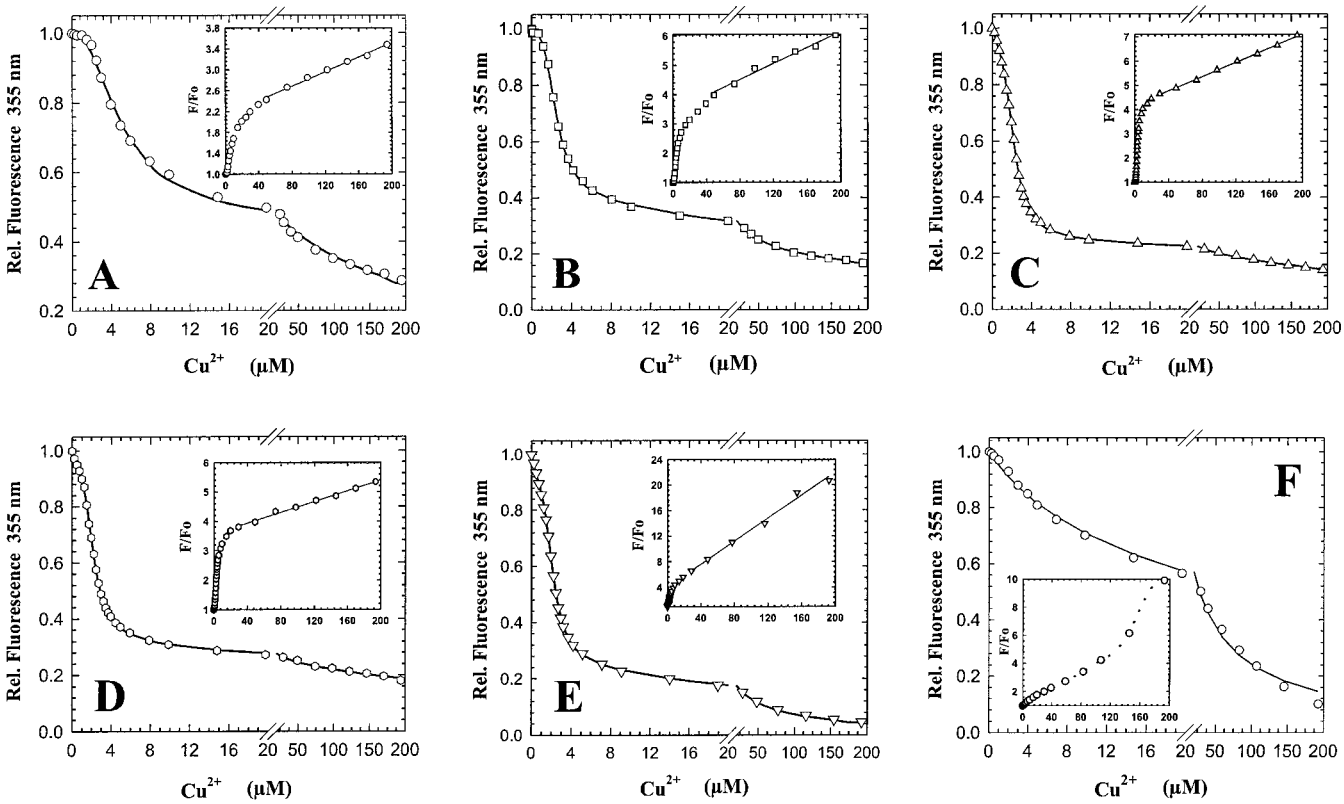

FIG. 4. **Fluorescence titration curves of the prion protein and its fragments with copper(II).** *A* shows the fluorescence data of 170 nM *hum*PrP_{60-91} (octarepeat), *B* of 145 nM *hum*PrP_{60-106}, *C* of 125 nM *hum*PrP_{23-98}, *D* of 120 nM *hum*PrP_{23-112}, *E* of 85 nM *mur*PrP_{23-231}, and *F* of 125 nM *mur*$PrP_{121-231}$. *Lines* represent the results of nonlinear regression analyses according to Equation 3. The *insets* represent Stern-Volmer plots of fluorescence data according to Equation 1. The result of linear regression analysis at high copper concentrations is indicated by a *straight line*.

spectra (Fig. 3*B*). The deconvoluted spectra showed molecular weight peaks for up to five bound copper on addition of 20–100 μM copper. In contrast to the preceding spectra (20, 40, 60, and 80 μM) there are only minor changes in the spectra going from 80 to 100 μM copper, suggesting a saturation of *mur*PrP_{23-231} with copper.

The average molecular masses for all used peptides and proteins are summarized in Table I. From this table the average mass differences between the copper sites almost corresponds to 61.5 amu, which is typically observed in copper(II) binding ESI mass spectrometry experiments. Because the average mass of copper is 63.5 amu, the difference of 2 amu is explained as displacement of two hydrogens on binding of each copper ion ($M + n{\cdot}Cu - 2{\cdot}n{\cdot}H^+$).

Comparing the results of *hum*PrP_{60-109}, *hum*PrP_{23-98}, and *hum*PrP_{23-112} only to *hum*PrP_{23-98}, an additional sixth copper ion appears to be bound. For *hum*PrP_{23-112}, which is almost identical to *hum*PrP_{23-98} but C-terminally extended, only five bound copper were observed. Also *hum*PrP_{60-109}, which shares an almost identical C-terminal extension to the octarepeat region, binds only five copper ions. Therefore the binding of a sixth copper ion to *hum*PrP_{23-98} appears to be an unspecific copper-binding site. Thus up to five copper ions appear to be bound specifically to *hum*PrP_{60-109}, *hum*PrP_{23-98}, and *hum*PrP_{23-112}, whereas four copper ions are bound to the octarepeat region, suggesting an additional copper-binding site within the N-terminal segment. Because the additional copper-binding site occurs already in *hum*PrP_{60-109}, which is compared with *hum*PrP_{60-91} C-terminally extended, this additional binding site has to be located C-terminally of the octarepeat region.

Fluorescence Titration of PrP^C and Its N-terminal Fragments with Copper—Fluorescence measurement and quantification of the copper binding to PrP^C and its fragments were difficult with respect to some items. First, to prevent unspecific binding of copper to PrP^C and its fragments, 100 mM NaCl was included. Second, to prevent unspecific aggregation and adsorption to surfaces 1 mM DTAC was added at a concentration clearly below critical micelle concentration (26). Third, for the quantification of affinities the peptide or PrP^C concentrations were chosen to be significantly lower than the dissociation constants, to assume that the free copper concentration is approximately equal to the added copper concentration. Fourth, in contrast to, *e.g.* calcium, the fluorescence of peptides and proteins is not only quenched by conformational changes induced by copper(II) binding but also by diffusion-controlled collision of copper(II) with tryptophan and tyrosine side chains (27–29). Thus fluorescence titration curves have to be recorded at copper concentrations far beyond the saturation point to get quantitative data from the fluorescence titration curves.

The fluorescence titration curves with copper(II) for the N-terminal fragments *hum*PrP_{60-91}, *hum*PrP_{60-109}, *hum*PrP_{23-98}, and *hum*PrP_{23-112}; the structured C-terminal fragment *mur*$PrP_{121-231}$; as well as for the full-length recombinant *mur*PrP_{23-231} are shown in Fig. 4, *A–F*. All curves, except that for *mur*$PrP_{121-231}$, show more or less clearly visible sigmoidal changes in fluorescence intensity upon addition of copper, suggesting a basic cooperative binding mechanism. It appears that the peptides/protein cannot be saturated with copper at high concentrations. This is due to collisional quenching, which can be shown by plots according to the Stern-Volmer equation (28),

$$F_o/F = 1 + K_{SV} \cdot [Q] \qquad \text{(Eq. 1)}$$

where F is the fluorescence at the individual concentration of the quencher $[Q]$ (which is copper in this case), F_o is the initial

TABLE II
Parameter for the dynamic and conformational fluorescence quenching of the prion protein and its N-terminal fragments by copper(II)

	K_{SV}[a]	f_{conf}[b]	K_{ind}[c]	f_{ind}[c]	K_{coop}[c]	f_{coop}[c]	n_{Hill}[c]
	M^{-1}		μM		μM		
humPrP_{60-91}	3230	0.53 (0.53)	—[d]	—[d]	5.5	0.53	2.4
humPrP_{60-109}	3980	0.71 (0.73)	8.8	0.25	2.5	0.48	3.7
humPrP_{23-98}	3490	0.76 (0.78)	1.4	0.19	2.2	0.58	3.6
humPrP_{23-112}	2560	0.72 (0.73)	2.4	0.25	2.2	0.48	3.7
murPrP_{23-231}	22500	0.75 (0.76)	1.8	0.28	2.2	0.48	4.2

[a] Data obtained by fitting with modified Stern-Volmer Equation 2.
[b] Data obtained by fitting to Equation 2 data in parentheses are the sum of f_{ind} and f_{coop}.
[c] Data obtained by fitting to Equation 3.
[d] Only cooperative sites were assumed and thus fitted without a mathematical term for an independent site (Equation 3).

fluorescence without quencher, and K_{SV} is the quenching constant also called the Stern-Volmer constant. Above the saturation point of copper binding to the peptides or protein, the changes of F_o/F should be linear in Stern-Volmer plots if this is only due to collisional quenching. Indeed, with the exception of *mur*$PrP_{121-231}$ (Fig. 4*F*, *inset*) the linearity in the Stern-Volmer plots of PrP^C and its N-terminal fragments (Fig. 4, *A*—*E*, *insets*) showed that the fluorescence changes above ~30–50 μM are the result of collisional quenching. The nonlinearity of the Stern-Volmer plot for *mur*$PrP_{121-231}$ might be explained by the different excitation wavelength of 285 nm instead of 295 nm used for reasons of sensitivity. The fluorescence of *mur*$PrP_{121-231}$, which has 11 tyrosines and only 1 tryptophan, probably reflects not only the Trp fluorescence but also the fluorescence of tyrosines, which are expected to have different dynamic copper-quenching properties.

From these Stern-Volmer plots, the Stern-Volmer constants as well as the fraction of conformational fluorescence change caused by binding of copper f_{conf} are calculated by linear regression analysis at high copper concentrations. For this purpose Equation 1 has to be modified, because it is only valid where exclusively collisional quenching occurs. In the presence of conformational fluorescence changes true values for K_{SV} can be calculated, introducing a correction factor according to Equation 2.

$$F_o/F = (1 + K_{SV} \cdot [Q])/(1 - f_{conf}) \quad \text{(Eq. 2)}$$

where f_{conf} is the fraction of conformational fluorescence changes. Thus to obtain the true value for K_{SV} the slopes from the Stern-Volmer plots have to be divided by the value of the ordinate $1/(1 - f_{conf})$. The Stern-Volmer plots yield values for f_{conf} and K_{SV} (Table II). The Stern-Volmer constant is used later to fit fluorescence data by nonlinear regression to obtain copper binding data. The values for K_{SV} represent a measure for the accessibility of tryptophan residues. For *hum*PrP_{60-109}, *hum*PrP_{23-98}, and *hum*PrP_{23-112}, K_{SV} decreases from almost 4000 M^{-1} to about 2500 M^{-1}, suggesting that the tryptophans become more buried in the holopeptides with longer fragment size. The reason for the at least 5–10-fold higher value for *mur*PrP_{23-231} is not known but has to be an effect of the C-terminal domain. Although the Stern-Volmer plot of *mur*$PrP_{121-231}$ (Fig. 4*F*, *inset*) could not be fitted very well with Equation 2, a similar Stern-Volmer constant of 22,000 M^{-1} could be estimated considering only data from 30 to 80 μM copper.

From the fluorescence titration curves (Fig. 4, *A*–*E*) it is apparent that there is a significant increase in affinity for copper(II) going from *hum*PrP_{60-91} (Fig. 4*A*) to *hum*PrP_{60-109} (Fig. 4*B*). Again a small increase in affinity can be observed going further to *hum*PrP_{23-98} (Fig. 4*C*), whereas the affinities of *hum*PrP_{23-98} and *hum*PrP_{23-112} (Fig. 4*D*), as well as for the full-length recombinant *mur*PrP_{23-231} (Fig. 4*E*) seem to be identical.

To get quantitative copper binding data the titration curves were fitted by nonlinear regression analysis. ESI mass spectrometry has confirmed that four copper ions bind to the octarepeat region (*hum*PrP_{60-91}). The mass spectrometry data suggest that one additional copper binding site exists for *hum*PrP_{60-109}, *hum*PrP_{23-98}, *hum*PrP_{23-112}, and *mur*PrP_{23-231}. This site was assumed to be independent, because particularly the titration curves for *hum*PrP_{23-98}, *hum*PrP_{23-112}, and *mur*PrP_{23-231} could only be fitted with a mathematical term for an independent binding site. Assuming almost equal fluorescence changes per cooperative binding site, data of titration curves were fitted according to Equation 3,

$$F_{rel} = \{1 - f_{ind} \cdot [Cu^{2+}]/(K_{ind} + [Cu^{2+}]) - f_{coop} \cdot [Cu^{2+}]^n/((K_{coop})^n + [Cu^{2+}]^n)\}/(1 + K_{SV} \cdot [Cu^{2+}]) \quad \text{(Eq. 3)}$$

where F_{rel} is the relative fluorescence; f_{ind} and K_{ind} are the fraction of fluorescence change and the dissociation constant for the independent binding site, respectively; f_{coop}, K_{coop}, and n are the fractional fluorescence change, the dissociation constant, and the Hill coefficient for the four cooperative binding sites, respectively; K_{SV} is the Stern-Volmer constant; and $[Cu^{2+}]$ is the free copper concentration. Because the peptide/protein concentration was chosen to be significantly lower than the dissociation constants, the added or total copper concentration was assumed to be equal to the free copper concentration. For the fitting procedure the Stern-Volmer constants obtained from Stern-Volmer plots were inserted for K_{SV} in Equation 3. Equation 3 was applied to all fluorescence titration curves except for *hum*PrP_{60-91}, because only cooperative binding sites were assumed, and thus the term for the independent site was omitted. The same held for *mur*$PrP_{121-231}$, but n was set to 1, because mass spectrometry suggested binding of only one copper ion, and thus no cooperative binding can occur.

The quantitative data (Table II) show that C- and N-terminal extensions in the sequence of the octarepeat region *hum*PrP_{60-91} have a significant influence on both dissociation constant K_{coop} and Hill coefficient n. The dissociation constants for the cooperative binding of four copper ions to the octarepeat region decrease significantly from 5.5 to 2.5 μM for *hum*PrP_{60-91} and finally only slightly to 2.2 μM for *hum*PrP_{23-98}, *hum*PrP_{23-112}, and *mur*PrP_{23-231}. Also Hill coefficients significantly increase from 2.4 to values ranging from 3.6 to 4.2 for *hum*PrP_{60-109}, *hum*PrP_{23-98}, *hum*PrP_{23-112}, and *mur*PrP_{23-231}, suggesting almost perfect cooperativity for the four cooperative copper-binding sites in the full-length prion protein. Similar changes in the dissociation constant are observed for the independent binding site. Here the values for K_{ind} significantly decreases from 8.8 μM to values between 1.4 and 2.4 μM for *hum*PrP_{23-98}, *hum*PrP_{23-112}, and *mur*PrP_{23-231}.

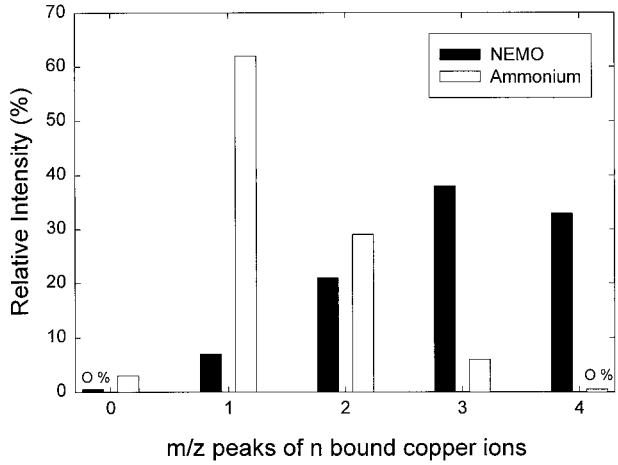

FIG. 5. **Relative population of the individual copper binding sites for the ESI mass spectra of *hum*PrP$_{60-91}$ for different buffers.** The spectra were recorded from either NEMO or an ammonium-containing buffer at pH 7.4 at a final concentration of 1 mM. 100 μM copper sulfate was added to 18 μM peptide.

For the one putative copper-binding site in *mur*PrP$_{121-231}$, a dissociation constant of about 8 μM was estimated considering that no precise mathematical fitting was obtained (see Fig. 4*F*).

DISCUSSION

Here we present for the first time affinity and stoichiometry data on the copper binding to *hum*PrP$_{60-109}$, *mur*PrP$_{121-231}$, and the full-length prion protein *mur*PrP$_{23-231}$ under physiological conditions as well as for *hum*PrP$_{23-112}$ representing a natural cleavage product of the prion protein (30, 31). Our results clearly demonstrate that the full-length prion protein binds copper within the physiological concentration range with binding of five copper ions per molecule. Furthermore, we proved that the positive cooperativity of copper binding is not restricted to N-terminal fragments but is a property of the full-length protein. The systematical comparison of the data for full-length PrP with C- and N-terminal fragments indicates that the N-terminal segment represents the cooperative copper-binding domain of the prion protein.

Mass spectrometry has evolved as a method in the assessment and elucidation of copper and heavy metal binding stoichiometry of proteins and peptides (32, 33). In contrast to Whittal *et al*. (34) we used ESI MS only for the copper binding stoichiometry studies for several reasons. First, our fluorescence affinity data indicated the copper binding sites of the prion protein and its fragments to be almost saturated with copper under the chosen concentrations in ESI MS. Therefore, it is expected to obtain mass spectra where predominantly the four or five copper adduct peaks are observed. This is not the case as readily visible from the spectra (see Fig. 2). It might be explained by the high flexibility of the N-terminal copper binding domain and thus its higher sensitivity to mechanical stress during the spraying procedure than more classical copper binding domains in which the copper binding sites are surrounded by several stabilizing secondary structure elements (35). Thus the ESI mass spectra appear not to reflect quantitatively the situation in solution but rather qualitatively for the prion protein and its peptides. Second, further investigations showed that ESI spectra are quite sensitive to changes of buffer and additives. The effect of ammonium salts on the ESI mass spectra of *hum*PrP$_{60-91}$ compared with NEMO as buffer is shown in Fig. 5. In contrast to the ammonium buffer system the third and fourth copper-binding sites are significantly populated using the *N*-ethylmorpholine instead. Additionally, the use of Tris with a functional primary amine prevented copper binding to *hum*PrP$_{58-91}$ in CD spectroscopy experiments (17). Summarized, ESI mass spectrometry of copper binding to prion protein and peptides appears to be quite sensitive to the chosen buffer and additive conditions. Therefore we have introduced *N*-ethylmorpholine as new buffer system in ESI mass spectrometry for metal interaction studies at a physiological pH of 7.

Our finding that the octarepeat region (*hum*PrP$_{60-91}$) binds four copper ions confirmed earlier mass spectrometry (13, 34) and circular dichroism spectroscopy data (17). The mass spectra of *hum*PrP$_{60-109}$, *hum*PrP$_{23-98}$, and *hum*PrP$_{23-112}$ revealed one additional copper-binding site. This is in good agreement with the binding of 5.6 copper(II) ions to *hum*PrP$_{23-98}$ from our earlier equilibrium dialysis experiments (18). From these experiments, as well as from the mass spectrum of *hum*PrP$_{23-98}$ (Fig. 2*C*), a sixth binding site, which was also observed earlier (34), might be assumed. But because only five copper ions were observed for *hum*PrP$_{60-109}$ and *hum*PrP$_{23-112}$, this site has to be unspecific. The involvement of the N-terminal amino group of *hum*PrP$_{23-98}$ for the unspecific site was proved by N-terminal acetylation (34).

Mass spectrometry data showed binding of up to five copper ions to the full-length protein, confirming one additional copper-binding site compared with the four of the octarepeat region. The data for the structured C-terminal domain *mur*PrP$_{121-231}$ containing three histidine residues revealed one possible copper-binding site with an estimated dissociation constant of 8 μM. This affinity is probably too low to be of physiological significance. For copper dissociation constants in the micromolar range, at least two side chains are essential from which one has to be a histidine or cysteine residue (36). Looking for this site in the three-dimensional NMR structure of the C-terminal fragment, we found a site made up of His^{140}, Asp^{147}, and Met^{138}. These residues are on the surface and close enough to each other (distance: ~5 Å).

In contrast to the putative C-terminal copper(II)-binding site for the fifth binding site in *hum*PrP$_{23-98}$, *hum*PrP$_{23-112}$, and full-length prion protein, we obtained a dissociation constant of about 2 μM. Since the additional fifth copper is already bound by *hum*PrP$_{60-109}$, it has to occur C-terminal of the octarepeat region. This binding site might be located at His^{96}, because it is known that besides the cysteine residue, the histidyl side chain is the major copper-binding site in peptides and proteins (36). In structured proteins at least two ligands, *e.g.* two histidine side chains, are necessary for copper binding in the micromolar concentration range (37). In flexible peptides without secondary structure only one histidine is essential for the copper binding. In such peptides the peptide backbone can adopt conformations in which peptide bond nitrogen is involved as a ligand in copper binding after deprotonation (38). Histidine hinders deprotonation of peptide bonds in the C-terminal position but promotes the deprotonation of N-terminally located peptide bonds as for *N*-acetyl-Gly-Gly-Gly-His (36). In this tetrapeptide the abstraction of the three adjacent peptide-bond hydrogens, together with the imidazole nitrogen, results in a 4N coordinated copper complex. The sequence at His^{96} . . . -Gly-Gly-Gly-Thr-His- . . . is strikingly similar to *N*-acetyl-Gly-Gly-Gly-His, but also His^{112} might be involved in copper binding. Further investigations are required to clarify the role of His^{96}, His^{112}, or His^{140} in the copper binding of prion protein.

The sigmoidal form of fluorescence titration curves for the prion protein and its N-terminal fragments clearly indicated an underlying positive cooperative binding mechanism. This agreed well with CD spectroscopy data for *hum*PrP$_{58-91}$, which is almost identical to our octarepeat fragment *hum*PrP$_{60-91}$ (17). In contrast, Whittal *et al.* (34) have obtained individual dissociation constants for *hum*PrP$_{58-91}$ clearly indicating a

negative cooperativity. This is probably explained by the limitations of ESI mass spectrometry in quantitative analysis and the buffer conditions as discussed above. Our results demonstrate that the positive cooperative copper binding is not restricted to the octarepeat fragment but is a general feature of the full-length prion protein.

The fluorescence data for $hum\mathrm{PrP}_{60-91}$ yielded a cooperative dissociation constant of 5.5 μM, which is almost identical to the value of 6 μM for $hum\mathrm{PrP}_{58-91}$ obtained by CD spectroscopy (17). Compared with equilibrium dialysis experiments for $hum\mathrm{PrP}_{23-98}$ with a dissociation constant of 5.9 μM (18), we have calculated significantly lower dissociation constants of 2.2 and 1.4 μM for the cooperative and the assumed independent site, respectively. This might be explained by the different experimental conditions. Our affinity data for $hum\mathrm{PrP}_{60-91}$ and $hum\mathrm{PrP}_{23-98}$ are difficult to compare with those obtained by quantitative ESI MS (34) for the already mentioned reasons and because we have obtained one cooperative constant instead of four individual constants from which only two were calculable in the case of $hum\mathrm{PrP}_{23-98}$ (34).

The similarity of the fluorescence titration curves of $hum\mathrm{PrP}_{23-98}$ and $hum\mathrm{PrP}_{23-112}$ with the full-length prion protein $mur\mathrm{PrP}_{23-231}$ as well as the obtained data (Table II) indicated that the N-terminal segment is a copper-binding domain. The putative low affinity copper-binding site in the C-terminal domain ($mur\mathrm{PrP}_{121-231}$) apparently had no influence on the copper-binding mode and affinity of the N-terminal segment. Although the total N-terminal segment up to amino acid 126 is highly flexible, C- and N-terminal extensions of the octarepeat region ($hum\mathrm{PrP}_{60-91}$) have a significant influence on the affinity and cooperativity of the independent and cooperative binding sites, respectively. They clearly increase if the octarepeat region is C-terminally extended to $hum\mathrm{PrP}_{60-109}$ (Table II). The affinity of the assumed independent site becomes significantly higher on N-terminal sequence extension from $hum\mathrm{PrP}_{60-109}$ to $hum\mathrm{PrP}_{23-98}$ or $hum\mathrm{PrP}_{23-112}$. Thus the fluorescence data of the four cooperative sites as well as for the assumed independent site indicated that there are additional interactions stabilizing the holocopper-binding domain.

Fluorescence titration curve data show that the full-length $mur\mathrm{PrP}_{23-231}$ is almost saturated at about 5 μM copper(II). This is within the physiological concentration range of the total copper concentration in blood plasma of 18.6 μM (39). But this concentration does not represent the physiologically available copper pool, because about 10.2 μM copper (65%) is bound to ceruloplasmin in a nonexchangeable way. In contrast about 2.8 μM is bound to serum albumin, 1.9 μM to transcuprein, and 3.6 μM is bound to low molecular weight components like amino acids in an exchangeable way. Considering only the copper pool of 3.6 μM bound by low molecular weight components and the copper affinities of the prion protein, there is strong argument for a direct role of the prion protein in copper metabolism. Additionally, copper concentrations ranging from 0.5 to 2.5 μM are found in the cerebrospinal fluid, whereas 15 μM is present in the synaptic cleft (40). In contrast to blood plasma the conditions at the synaptic cleft and in the cerebrospinal fluid are probably different in that no ceruloplasmin, serum albumin, or transcuprein is present.

The cooperative copper-binding mode of the prion protein within the physiological concentration range suggests two possible functions. First, similar to the cooperative oxygen binding of hemoglobin, it might play a role in copper transport. Second, the prion protein might be a copper sensor similar to the intracellular calcium-binding protein calmodulin, which also binds calcium in a cooperative way.

In mammals, relatively little is currently known about the precise components involved in copper transport and the mechanism by which copper is transported across the plasma membrane into cells (41). Cellular copper uptake by the prion protein might be similar to transferrin, which is mediated by endocytosis. Both transferrin and prion protein release their bound iron and copper at an acidic pH of 5.0 (15). A possible transport function for PrP^C is supported by the stimulation of endocytosis with copper (42), the pH-dependent copper binding (17), and the lower copper content of brain in PrP^C-deficient mice (18). This was recently further supported by our results showing that PrP^C is apparently located in presynaptic membranes and that the loss of PrP^C in $Prnp^{0/0}$ mice strongly affected the copper content of synaptosomes (14). This suggests that PrP^C is involved in the synaptic copper homeostasis.

The *in vivo* binding mode of copper to the prion protein is not yet known. Even if PrP^C does not bind copper under normal conditions, it might serve as an extracellular copper sensor. It is known that cancer and infections increase plasma copper concentrations in blood (39). Thus it might be that PrP^C binds copper and regulates cells on increasing copper concentration.

Copper binding to PrP appears to play a role in the prion disease as well (43). Copper apparently stabilized prions, because it enhances the regeneration of partially denatured PrP^{Sc} (5). Our finding of a low affinity copper-binding site in the C-terminal domain of PrP^C might be interesting for the conformational change to PrP^{Sc}.

Further investigations are necessary to explore the molecular nature of the unique, cooperative, copper binding motif in the octarepeat region as well as to elucidate the role of copper binding for the prion protein *in vivo*.

Acknowledgment—We thank Prof. Hübner for critically reading the manuscript, Dr. Nietmann for the use of HPLC, and K. Kroll for the use of fluorescence spectrophotometer. Furthermore, we thank Tanja Wucherpfennig for assistance in expression of $hum\mathrm{PrP}_{23-98}$ and Meike Barche for excellent technical assistance.

REFERENCES

1. Pan, K.-M., Baldwin, M., Nguyen, J., Gasset, M., Serban, A., Groth, D., Mehlhorn, I., Ziwei, H., Fletterick, R. J., Cohen, F. E., and Prusiner, S. B. (1993) *Proc. Natl. Acad. Sci. U. S. A.* **90,** 10962–10966
2. Post, K., Pitschke, M., Schäfer, O., Wille, H., Appel, T. R., Kirsch, D., Mehlhorn, I., Serban, H., Prusiner, S. B., and Riesner, D. (1998) *Biol. Chem.* **379,** 1307–1317
3. McKinley, M. P., Bolton, D. C., and Prusiner, S. B. (1983) *Cell* **35,** 57–62
4. Büeler, H., Fischer, M., Lang, Y., Bluethmann, H., Lipp, H.-P., DeArmond, S. J., Prusiner, S. B., Auet, M., and Weissmann, C. (1992) *Nature* **356,** 577–582
5. McKenzie, D., Bartz, J., Mirwald, J., Olander, D., Marsh, R., and Aiken, J. (1998) *J. Biol. Chem.* **273,** 25545–25547
6. Bendheim, P. E., Brown, H. R., Rudelli, R. D., Scala, L. J., Goller, N. L., Wen, G. Y., Kascsak, R. J., Cashman, N. R., and Bolton, D. C. (1992) *Neurology* **42,** 149–156
7. Stahl, N., Borchelt, D. R., and Prusiner, S. B. (1990) *Biochemistry* **29,** 5405–5412
8. Riek, R., Hornemann, S., Wider, G., Billeter, M., Glockshuber, R., and Wüthrich, K. (1996) *Nature* **382,** 180–182
9. Riek, R., Hornemann, S., Wider, G., Glockshuber, R., and Wüthrich, K. (1997) *FEBS Lett.* **413,** 282–288
10. Donne, D. G., Viles, J. H., Groth, D., Mehlhorn, I., James, T. L., Cohen, F. E., Prusiner, S. B., Wright, P. E., and Dyson, H. J. (1997) *Proc. Natl. Acad. Sci. U. S. A.* **94,** 13452–13457
11. Büeler, H., Aguzzi, A., Sailer, A., Greiner, R.-A., Autenried, P., Aguet, M., and Weissmann, C. (1993) *Cell* **73,** 1339–1347
12. Lledo, P. M., Tremblay, P., DeArmond, S. J., Prusiner, S. B., and Nicoll, R. A. (1996) *Proc. Natl. Acad. Sci. U. S. A.* **93,** 2403–3407
13. Hornshaw, M. P., McDermott, J. R., and Candy, J. M. (1995) *Biochem. Biophys. Res. Commun.* **207,** 621–629
14. Herms, J., Tings, T., Gall, S., Madlung, A., Giese, A., Siebert, H., Schürrmann, P., Windl, O. Brose, N., and Kretzschmar, H. (1999) *J. Neurosci.* **19,** 8866–8875
15. Stöckel, J., Safar, J., Wallace, A. C., Cohen, F. E., and Prusiner, S. B. (1998) *Biochemistry* **37,** 7185–7193
16. Hornshaw, M. P., McDermott, J. R., Candy, J. M., and Lakey, J. H. (1995) *Biochem. Biophys. Res. Commun.* **214,** 993–999
17. Viles, J. H., Cohen, F. E., Prusiner, S. B., Goodin, D. B., Wright, P. E., and Dyson, H. J. (1999) *Proc. Natl. Acad. Sci. U. S. A.* **96,** 2042–2047
18. Brown, D. R., Qin, K., Herms, J. W., Madlung, A., Manson, J., Strome, R., Fraser, P. E., Kruck, T., von Bohlen, A., Schulz-Schaeffer, W., Giese, A., Westaway, D., and Kretzschmar, H. (1997) *Nature* **390,** 684–687

19. Coste, J., Le-Nguyen, D., and Castro, B. (1990) *Tetrahedron Lett.* **31,** 205–208
20. Windl, O., Dempster, M., Estibeiro, J. P., Lathe, R., de Silva, R., Esmonde, T., Will, R., Springbett, A., Campbell, T. A., Sidle, K. C. L., Palmer, M. S., and Collinge, J. (1996) *Hum. Genet.* **98,** 259–264
21. Liemann, S., and Glockshuber, R. (1999) *Biochemistry* **38,** 3258–3267
22. Hornemann, S., and Glockshuber, R. (1996) *J. Mol. Biol.* **262,** 614–619
23. Birdsall, B., King, R. W., Wheeler, M. R., Lewis, C. A., Goode, S. R., Dunlap, R. B., and Roberts, G. C. K. (1983) *Anal. Biochem.* **132,** 353–361
24. Gill, S. C., and von Hippel, P. H. (1989) *Anal. Biochem.* **182,** 319–326
25. Sandmeier, E., Hunziker, P., Kunz, B., Sack, R., and Christen, P. (1999) *Biochem. Biophys. Res. Commun.* **261,** 578–583
26. Hjelmeland, L. M. (1986) *Methods Enzymol.* **124,** 135–164
27. Syvertsen, C., Melö, T. B., and Ljones, T. (1987) *Biochim. Biophys. Acta* **914,** 6–18
28. Chen, R. F. (1976) in *Biochemical Fluorescence: Concepts* (Chen, R. F., and Edelhoch, H., eds) pp. 573–606, Marcel Dekker, Inc., New York
29. Eftink, M. R., and Ghiron, C. A. (1981) *Anal. Biochem.* **114,** 199–227
30. Caughey, B., Raymond, G. J., Ernst, D., and Race, R. E. (1991) *J. Virol.* **65,** 6597–6603
31. Chen, S. G., Teplow, D. B., Parchi, P., Teller, J. K., Gambetti, P., and Autilio-Gambetti L. (1995) *J. Biol. Chem.* **270,** 19173–19180
32. Loo, J. A. (1997) *Mass Spectrom. Rev.* **16,** 1–23
33. Mann, M., and Wilm, M. (1995) *Trends Biochem. Sci.* **20,** 219–224
34. Whittal, R. M., Ball, H. L., Cohen, F. E., Burlingame, A. L., Prusiner, S. B., and Baldwin, M. A. (2000) *Protein Sci.* **9,** 332–343
35. Adman, E. T. (1991) *Adv. Protein Chem.* **42,** 145–197
36. Sovago, I. (1990) in *Biocoordination Chemistry/Coordination Equilibria in Biologically Active Systems* (Burger, K., ed) pp. 135–184, Ellis Horwood Limited, New York
37. Regan, L. (1995) *Trends Biochem. Sci.* **20,** 280–285
38. Regan, L. (1993) *Annu. Rev. Biophys. Biomol. Struct.* **22,** 257–281
39. Linder, M. C., and Hazegh-Azam, M. (1996) *Am. J. Clin. Nutr.* **63,** 797S–811S
40. Hartter, D. E., and Barnea, A. (1988) *J. Biol. Chem.* **263,** 799–805
41. Vulpe, C. D., and Packman, S. (1995) *Annu. Rev. Nutr.* **15,** 293–322
42. Paul, P. C., and Harris, D. A. (1998) *J. Biol. Chem.* **273,** 33107–33110
43. Wadsworth, J. D., Hill, A. F., Joiner, S., Jackson, G. S., Clarke, A. R., and Collinge, J. (1999) *Nat. Cell Biol.* **1,** 55–59

Prion Protein Binds Copper within the Physiological Concentration Range

Michael L. Kramer, Hartmut D. Kratzin, Bernhard Schmidt, Alice Römer, Otto Windl, Susanne Liemann, Simone Hornemann and Hans Kretzschmar

J. Biol. Chem. 2001, 276:16711-16719.
doi: 10.1074/jbc.M006554200 originally published online February 27, 2001
